FARADAY

Formation of HO_2 from OH and C_2H_2 in the presence of O_2

Birger Bohn† and Cornelius Zetzsch*

Fraunhofer-Institut für Toxikologie und Aerosolforschung, Nikolai-Fuchs-Strasse 1, D-30625 Hannover, Germany

Pulsed production of OH in a gas-phase system containing acetylene, O_2 and NO resulted in biexponential OH-decay curves, indicating formation of HO_2 in secondary reactions. Production and detection of OH were performed by 248 nm photolysis of H_2O_2 and cw-laser long-path absorption at 308 nm, respectively. Measurements were made at room temperature in O_2 or N_2–O_2 mixtures containing 5% O_2 at total pressures between 10 and 100 kPa. Analysis of the decay curves resulted in effective rate constants for the removal of OH and the formation of HO_2 by acetylene in the presence of O_2 in the range $(1.4–3.5) \times 10^{-13}$ $cm^3\ s^{-1}$, dependent on total pressure and O_2 concentration. HO_2 is thought to be formed from HCO and O_2, with HCO originating in a reaction of an intermediate acetylene–OH adduct with O_2. HO_2 yields were found to vary between 1.13 and 1.01 and tending to higher values at lower total pressures. These yields are higher than the expected value of 1, which can be explained by a dissociation of a small fraction of vibrationally excited glyoxal formed, together with OH in a second channel of the acetylene–OH adduct + O_2 reaction. In order to check whether the increased HO_2 yields are real, CO was used instead of acetylene. In this case, an HO_2 yield of 0.99 was found, in good agreement with expectations, and a rate constant of $(1.66 \pm 0.25) \times 10^{-13}$ $cm^3\ s^{-1}$ for the OH + CO reaction in 20 kPa O_2 was determined. In addition, a rate constant for the HO_2 + NO reaction of $(9.5 \pm 1.5) \times 10^{-12}$ $cm^3\ s^{-1}$, rate constants for the OH + NO reaction in the range $(1.3–7.4) \times 10^{-12}$ $cm^3\ s^{-1}$, depending on total pressure, and upper limits for the rate constants of possible reactions $HO_2 + C_2H_2$ ($k \leqslant 5 \times 10^{-15}$ $cm^3\ s^{-1}$) and HO_2 + CO ($k \leqslant 3 \times 10^{-15}$ $cm^3\ s^{-1}$) were derived. Error limits include statistical (2σ) and possible systematic errors.

Reaction with OH radicals is the dominant process determining the tropospheric lifetime of many natural and anthropogenic trace gases. Often, this primary oxidation step leads to a formation of HO_2 in secondary reactions and OH can be recovered by reaction of HO_2 with NO. This cycle is essential for the self-cleaning capacity of the atmosphere. In some cases HO_2 formation occurs almost instantaneously in secondary reactions with atmospheric oxygen, for example that of H atoms from the reaction of OH with CO. However, HO_2 is often a product of reaction sequences *via* organic peroxyl radicals, RO_2, involving O_2 and NO. In these cases the HO_2 formation is delayed, and competitive channels leading to losses in the radical chain are possible.

Acetylene oxidation is initiated by pressure-dependent addition of OH (1a),[1–13] which, at low pressure, competes with a bimolecular channel (1b) forming ketene,[14–16]

$$OH + C_2H_2 \xrightarrow{M} C_2H_2OH \quad (1a)$$

$$\longrightarrow CH_2CO + H \quad (1b)$$

while abstraction of H atoms is unimportant at room temperature.[5,6] In the presence of oxygen, part of the OH consumed in reaction (1a) can be regenerated directly (*i.e.* not *via* HO_2) by a reaction of the adduct, C_2H_2OH, with O_2.[8–13] Recently, we have shown that the OH yield of this reaction depends strongly on the O_2 mixing ratio but not on the total pressure.[13] Smog chamber investigations by Hatakeyama *et al.*,[17] performed in synthetic air at atmospheric pressure, showed that glyoxal, $(CHO)_2$, and formic acid, HCO_2H, are the major stable products formed following acetylene reaction with OH. On the other hand, ketene could not be detected,[17] indicating that reaction (1b) is negligible at atmospheric pressure. The reported glyoxal yield of 0.7 ± 0.3 [17] is similar to our OH yield observed under the same conditions,[13] 0.70 ± 0.04, supporting the reaction paths proposed for the acetylene–OH adduct + O_2 reaction:[17]

$$C_2H_2OH + O_2 \rightarrow (CHO)_2 + OH \quad (2a)$$

$$\rightarrow HCO_2H + HCO \quad (2b)$$

However, a change in the yields of the stable products $(CHO)_2$ and HCO_2H as a function of the O_2 mixing ratio, as expected from our work on the OH yield, has not yet been investigated. In this work, in addition to looking for OH formed in reaction (2a), we detect HCO formed in reaction (2b) by converting it into HO_2,

$$HCO + O_2 \rightarrow HO_2 + CO \quad (3)$$

and finally OH:

$$HO_2 + NO \rightarrow OH + NO_2 \quad (4)$$

In this way it is possible to check whether the observed change in the OH yield from reaction (2) with the O_2 mixing ratio corresponds to a matching change in the yield of HCO *i.e.* whether the total amount of radicals formed in reaction (2) stays constant while the total pressure or O_2 mixing ratio are changed.

The basic idea of extracting quantitative information on the HCO yield from OH-decay curves is that, with high levels of O_2, steady-state conditions can be maintained for both C_2H_2OH and HCO. As a consequence, a pulsed production of OH results in an OH time-behaviour similar to that observed if HO_2 were formed directly in the initiating OH + C_2H_2 reaction. Such a system has recently been examined in our laboratory,[18] namely the reaction of OH with H_2O_2,

$$OH + H_2O_2 \rightarrow H_2O + HO_2 \quad (5)$$

followed by reaction (4) to recover OH, while the radical chain was terminated by reaction of OH with NO:

$$OH + NO \xrightarrow{M} HONO \quad (6)$$

In this work we have extended this former reaction scheme (4)–(6) by addition of acetylene and O_2. From an analysis of

† Present address: Physical and Theoretical Chemistry Laboratory, South Parks Road, Oxford, OX1 3QZ, UK.

the resulting biexponential OH-decay curves, the yield of HO_2 (*i.e.* of HCO in the presence of O_2) formed for each OH effectively consumed in reactions (1) and (2) can be determined.

Additional measurements were performed with CO instead of C_2H_2, in order to test this scheme. In this case, reaction with OH leads to formation of H atoms,

$$OH + CO \rightarrow H + CO_2 \quad (7)$$

which are also rapidly converted into HO_2 under the experimental conditions employed.

$$H + O_2 \xrightarrow{M} HO_2 \quad (8)$$

Thus, steady-state conditions can be assumed for the H atoms, which qualitatively leads to the same time-behaviour for OH. However, an HO_2 yield of one is strictly expected in this simpler reaction chain.

Experimental

Measurements were made in a 20 l glass tube designed for time-resolved detection of OH by cw-laser long-path absorption at 308 nm. An excimer laser was used for pulsed production of OH by 248 nm photolysis of H_2O_2. This experimental set-up is described in more detail elsewhere.[8,9,13,18]

Gas mixtures of known composition were slowly flowing (*ca.* 3 l min^{-1} STP) through the reaction cell at room temperature (296 ± 2 K). H_2O_2 concentrations were varied in the range 0.8–2.7 Pa, leading to OH starting concentrations of, typically, 5×10^{10} cm^{-3}. This is more than three orders of magnitude less than the lowest reactant concentrations used. Thus, pseudo-first-order conditions are assumed to be valid for OH. H_2O_2 concentrations are maintained by purging a concentrated liquid solution with a constant flow of N_2 or O_2.[13] Since H_2O_2 decomposes to some extent by wall reactions in the cell,[13] actual concentrations were calculated by recording OH-decay curves before and after addition of other reactants. The measured decay rates (τ_0^{-1}) can be converted to H_2O_2 concentrations using literature data on the rate constant of the OH + H_2O_2 reaction.[19] The OH-decay rate coefficient in the absence of reactants is estimated[18] to be below 10 s^{-1}. Total pressures of 10, 20, 50 and 100 kPa, using either O_2 or an O_2–N_2 mixture containing 5% O_2 as matrix gases, were applied. However, owing to the use of diluted NO, 1–3% of rare gases (Ar or He) were always present. Reactant concentrations were calculated from the gas-flow rates, maintained by calibrated flow controllers, and total pressures.

The gases used had the following minimum purities (Messer Griesheim): N_2 99.999%, O_2 99.995%, NO 99.5%, C_2H_2 99.6%, CO 99.998%. NO was diluted in Ar (2000 ppm) or He (500 ppm) with concentrations precise to within 2% (Messer Griesheim). Before entering the cell, NO_2 traces were removed using a converter filled with solid iron(II) sulfate. C_2H_2 was available from Messer Griesheim in pure form (⩾99.6%) and diluted in He (5%). Since the diluted C_2H_2 was found to be contaminated with 4–6% of acetone (not stated by the manufacturer) such runs were discarded. On the other hand, we checked that the pure C_2H_2 contained less than 0.5% of acetone by means of gas chromatography.

Since the reaction chain initiated by OH is very effective, it may cause a decrease in reactant concentrations, especially of NO (see below). To prevent this, OH-decay curves were initially accumulated over no more than three laser shots. After this, 5–20 min were allowed to elapse to ensure an exchange of the largest part of the gas volume (⩾95%, assuming the reaction cell to behave like an ideal stirred reactor[13]) until the next measurement was started. To obtain reasonable OH-decay curves the absorption signals of 20–30 single laser shots were finally averaged. Fig. 1 shows a set of typical OH-decay curves obtained with different C_2H_2 concentrations. The time profiles are biexponential (a sum of two monoexponential decays) as will be discussed in more detail below. Decay-curve parameters were derived in non-linear least-squares fits, considering the amplitudes and time constants of the two exponentials and the background signal. However, the decay curves are affected by the time constant of the detection system, which causes a delayed increase in the absorption signal at very short times. As a consequence, data points collected at $t \leqslant 0.2$ ms were not considered in the fits, and the relative amplitudes of the two exponentials were corrected as outlined elsewhere.[18]

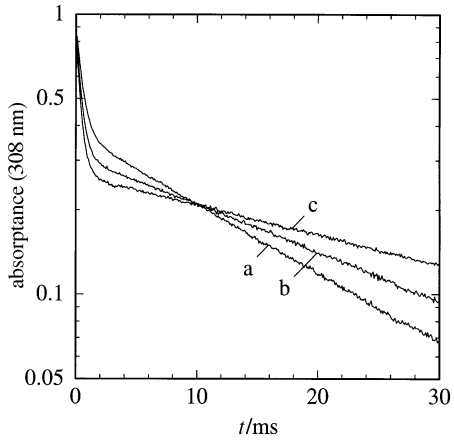

Fig. 1 Typical OH-decay curves obtained with different concentrations, $[C_2H_2]/10^{15}$ cm^{-3}: (a) 1.3, (b) 2.5, (c) 3.7. The measured absorptance, *i.e.* the ratio of absorbed and incident laser flux on the $Q_1(2)$ line of the OH (A–X) transition, is taken as a direct measure of the $[OH]/[OH]_0$. Experimental parameters as given in Table 1 (#12).

Table 1 gives a summary of experimental parameters employed in the experiments. Decay curves were recorded for five–nine different C_2H_2 or CO concentrations. For a given total pressure and O_2 level, these sets were performed with at

Table 1 Experimental parameters employed in the different sets of measurements: total pressures, C_2H_2 concentration ranges, and concentrations of NO and H_2O_2 (reflected in τ_0^{-1})

	p_{tot}/kPa	$[C_2H_2]$/[a] 10^{15} cm^{-3}	N[b]	[NO]/ 10^{14} cm^{-3}	τ_0^{-1}/[c] 10^2 s^{-1}
		matrix gas: 5% O_2 in N_2 [d]			
1	19.7	3.7	6	0.79	3.56
2	19.7	3.7	6	0.78	6.05
3	19.3	5.8	8	1.27	3.64
4	19.9	3.7	6	1.30	6.11
5	47.3	3.9	6	0.74	6.10
6	50.3	6.2	5	1.39	6.56
7	98.4	8.2	6	0.99	7.34
8	98.8	8.1	6	1.54	11.44
		matrix gas: O_2 [d]			
9	10.1	2.5	5	1.09	3.22
10	10.1	2.4	6	1.68	5.29
11	19.8	3.7	6	0.80	3.65
12	20.0	3.7	9	0.80	5.95
13	19.8	3.7	9	1.32	3.52
14	20.0	3.7	6	1.32	6.13
15	50.6	6.3	5	0.88	6.84
16	50.9	6.3	6	1.53	6.68
		matrix gas: O_2 [d], CO instead of C_2H_2			
17	21.5	18	8	1.12	6.31
18	20.0	17	6	1.80	6.01

[a] Maximum value of concentration range. [b] Total number of data points (*i.e.* of different C_2H_2 concentrations). [c] Measured before and after addition of NO and C_2H_2 (CO). [d] 1–3% of He or Ar are always present owing to the use of diluted NO.

least two different NO concentrations and, in some cases, different H_2O_2 concentrations, the latter being reflected in the different τ_0^{-1} values.

Results

Evaluation of rate constants and HO_2 yields

Production of OH in the present system is assumed to initiate a reaction chain as described in the introduction and shown in Fig. 2, neglecting reaction (1b), possibly leading to an HO_2 production *via* H + O_2 (see below). The concentrations of the radical species C_2H_2OH and HCO are presumed to be in a steady state,

$$\frac{d[C_2H_2OH]}{dt} = \frac{d[HCO]}{dt} = 0 \qquad \text{(I)}$$

which is justified considering the high concentrations of O_2 employed ($>10^{17}$ cm^{-3}) and the rate constants of the corresponding reactions with O_2 ($k_2 \approx k_3 \approx 5 \times 10^{-12}$ cm^3 s^{-1}).[12,19] For the loss and formation of OH and HO_2 the following system of differential equations remains:

$$\frac{d[OH]}{dt} = -{}^1k^{\text{eff}}_{1,\,OH}[OH] + {}^1k_{f,\,OH}[HO_2] \qquad \text{(II)}$$

$$\frac{d[HO_2]}{dt} = {}^1k^{\text{eff}}_{f,\,HO_2}[OH] - {}^1k_{1,\,HO_2}[HO_2] \qquad \text{(III)}$$

The four coefficients are pseudo-first-order rate constants (indicated by the index 1 and considered as effective on account of our simplifications). For the loss of OH we obtain:

$$\begin{aligned} {}^1k^{\text{eff}}_{1,\,OH} &= \left\{k_{1a}\left(1 - \frac{k_{2a}}{k_2}\right) + k_{1b}\right\}[C_2H_2] \\ &\quad + k_5[H_2O_2] + k_6[NO] \\ &= k^{\text{eff}}[C_2H_2] + c_{1,\,OH} \end{aligned} \qquad \text{(IV)}$$

Additional loss terms due to diffusion or impurities in the system are small ($\leqslant 10$ s^{-1}), as stated above, and not considered here. Assuming an OH yield of one for the HO_2 + NO reaction,[18] and that reaction with NO is the only loss process for HO_2, for which experimental evidence will be given below, the rate coefficients for formation of OH and loss of HO_2 are similar.

$${}^1k_{f,\,OH} = {}^1k_{1,\,HO_2} = k_4[NO] \qquad \text{(V)}$$

Finally, according to the reaction model, the effective rate coefficient for formation of HO_2 is expected to be given by the following equation.

$$\begin{aligned} {}^1k^{\text{eff}}_{f,\,HO_2} &= \left\{k_{1a}\frac{k_{2b}}{k_2} + k_{1b}\right\}[C_2H_2] + k_5[H_2O_2] \\ &= k^{\text{eff}}[C_2H_2] + c_{f,\,HO_2} \end{aligned} \qquad \text{(VI)}$$

Whether or not this equation describes the kinetics of HO_2 formation in the present system correctly will be examined below.

Integration[20] of eqn. (II) and (III) leads to the biexponential time dependence for OH that has been observed experimentally.

$$\frac{[OH](t)}{[OH]_0} = c_1 \exp(-t/\tau_1) + c_2 \exp(-t/\tau_2) \qquad \text{(VII)}$$

The decay curves in Fig. 1 demonstrate the contrasting influence of the C_2H_2 concentration on the time profiles. With increasing concentration the first (faster) time constant decreases while the second (slower) increases.

The parameters characterising the decays are related to the rate coefficients by the following equations (assuming $[HO_2]_0 = 0$).[18,20]

$${}^1k_{1,\,HO_2} = \frac{\tau_1^{-1} + \tau_2^{-1}c_1/c_2}{c_1/c_2 + 1} \qquad \text{(VIII)}$$

$${}^1k^{\text{eff}}_{1,\,OH} = \tau_1^{-1} + \tau_2^{-1} - {}^1k_{1,\,HO_2} \qquad \text{(IX)}$$

$${}^1k^{\text{eff}}_{f,\,HO_2}\,{}^1k_{f,\,OH} = {}^1k^{\text{eff}}_{1,\,OH}\,{}^1k_{1,\,HO_2} - \tau_1^{-1}\tau_2^{-1} \qquad \text{(X)}$$

The coefficients for formation of OH and HO_2 appear as a product in eqn. (X). However, they can be separated using the assumptions described above [*i.e.* eqn. (V)] which leads to:

$${}^1k^{\text{eff}}_{f,\,HO_2} = {}^1k^{\text{eff}}_{1,\,OH} - \frac{\tau_1^{-1}\tau_2^{-1}}{{}^1k_{1,\,HO_2}} \qquad \text{(XI)}$$

With eqn. (VIII), (IX) and (XI), HO_2 yields can be derived from the experimentally determined decay-curve parameters by comparing the corresponding rate coefficients for OH loss and HO_2 formation. Table 2 gives examples of typical biexponential curve parameters and their dependences on C_2H_2 concentrations, as well as the corresponding rate coefficients. No deviation from a biexponential time behaviour was noticeable for the experimental conditions listed in Table 1. However, measurements were also performed at a total pressure of 10 kPa with 5% O_2. Under these conditions, unusually high residuals were observed in the fits, especially at short reaction times, and HO_2 loss rate coefficients, significantly lower (*ca.* 70%) than for all other series, were derived. This inconsistency was only observed in the presence of C_2H_2. The proposed reaction model and/or the simplifications may, therefore, not be valid under these conditions, and the data will not be further considered in the Results section.

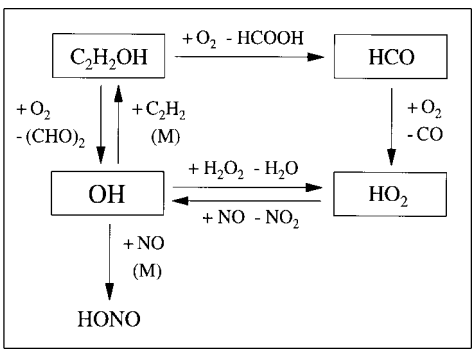

Fig. 2 Proposed reaction model[13,17,18]

Table 2 Biexponential curve parameters and resulting rate coefficients as a function of C_2H_2 concentration obtained within a typical set of measurements (#11)

$[C_2H_2]/10^{15}$ cm^{-3}	$\tau_1^{-1}/10^3$ s^{-1}	τ_2^{-1}/s^{-1}	c_1/c_2	${}^1k_{1,\,HO_2}/10^3$ s^{-1}	${}^1k^{\text{eff}}_{1,\,OH}/10^3$ s^{-1}	${}^1k^{\text{eff}}_{f,\,HO_2}/10^3$ s^{-1}
0.66	1.40	82	0.97	0.75	0.73	0.58
1.29	1.61	65	1.24	0.76	0.92	0.78
1.91	1.80	55	1.48	0.76	1.10	0.97
2.53	1.95	41	1.77	0.73	1.26	1.15
3.13	2.16	34	1.97	0.75	1.44	1.35
3.72	2.30	26	2.16	0.75	1.58	1.50

Additional experimental parameters are given in Table 1. A further analysis of the data can be found in Table 3.

Measurements with CO were carried out at a total pressure of 20 kPa of O_2, where the rate constant of the $H + O_2$ reaction is high enough ($k_8 \approx 2.5 \times 10^{-13}$ cm^3 s^{-1})[19] to assume steady-state conditions for H-atoms. Hence, replacing $k^{\text{eff}}[C_2H_2]$ by $k_7[CO]$ in eqn. (IV) and (VI) leads to the same expressions as derived above.

Rate constants of HO_2 reactions

Loss rate coefficients of HO_2 were obtained using eqn. (VIII). Since no noticeable dependence on C_2H_2 (or CO) concentrations was found, the results were averaged for the different sets, *i.e.* over five–nine single measurements. These averages are given in Table 3 with error limits indicating the largest deviations found within the sets. Hence, they reflect reproducibility rather than accuracy. Moreover, since no dependence on total pressure was apparent, the averaged data were combined in a plot *vs.* NO concentrations, to determine the $HO_2 + NO$ rate constant. A linear regression gave $k_4 = (9.5 \pm 0.5) \times 10^{-12}$ cm^3 s^{-1} ($\pm 2\sigma$) and an intercept close to zero (-15 ± 65 s^{-1}). These results are in good agreement with our recent study,[18] also showing the absence of any pressure effect on the rate constant. Moreover, the assumption that reaction with NO is the only loss process for HO_2 in the system appears to be justified. Possible systematic errors affecting the rate constant are estimated to be below 10%[18] leading to a total relative error of 15%.

In order to derive upper limits for rate constants of the possible reactions $HO_2 + C_2H_2$ and $HO_2 + CO$ the averaged HO_2 loss rate coefficients from Table 3 were subtracted from the single values and the differences plotted *vs.* C_2H_2 and CO concentration, respectively. From a linear regression to these data (a total of 101 and 14 data points, respectively) slightly negative slopes of (-0.5 ± 2.1) and $(-1.5 \pm 3.8) \times 10^{-15}$ cm^3 s^{-1} were obtained, corresponding to upper limits ($\pm 2\sigma$) for the rate constants of 1.6 and 2.3×10^{-15} cm^3 s^{-1}, respectively. These reactions obviously have no importance. However, the fact that the fitted slopes are negative, hints towards a small loss of NO in the radical chain. The same applies for the fitted intercept in the case of $HO_2 + NO$, as has been noticed in earlier work.[18]

The amount of NO consumed can be calculated by integrating by equation,

$$\frac{d[NO]}{dt} = -[NO](k_6[OH] + k_4[HO_2]) \qquad \text{(XII)}$$

with [OH] given by eqn. (VII) and $[HO_2]$ by eqn. (XIII),

$$\frac{[HO_2](t)}{[OH]_0} = c_3\{\exp(-t/\tau_2) - \exp(-t/\tau_1)\} \qquad \text{(XIII)}$$

where c_3 can be expressed in terms of the parameters given above:

$$c_3 = \sqrt{c_1 c_2 \frac{{}^1k^{\text{eff}}_{\text{f, HO}_2}}{{}^1k_{\text{f, OH}}}} \qquad \text{(XIV)}$$

Taking the experimental set from Table 2 as an example, the decrease in NO concentration caused by the initial production of 5×10^{10} cm^{-3} of OH was calculated to be 0.3% and 1.3% for the lowest and highest concentrations of C_2H_2, respectively. Averaging over three laser shots, as described above, this corresponds to an NO decrease of *ca.* 1.5% within the set, caused by the increase in C_2H_2. Considering the $HO_2 + NO$ rate constant, this is expected to lead to a decrease in the HO_2 loss rate coefficient of the order of 10 s^{-1}. Plotted *vs.* C_2H_2 concentration this will result in a slope of *ca.* -3×10^{-15} cm^3 s^{-1}, of the same order as the slopes determined experimentally. Considering this systematic deviation, the upper limit of the rate constant of a possible reaction $HO_2 + C_2H_2$ is estimated to be 5×10^{-15} cm^3 s^{-1}. In the case of CO this perturbation is less, since the amount of NO consumed is considerably less compared with C_2H_2 (see below). Hence, an upper limit of 3×10^{-15} cm^3 s^{-1} is estimated for the rate constant of a possible $HO_2 + CO$ reaction.

Effective rate constants of $OH + C_2H_2$ and rate constants of $OH + CO$

Effective OH-loss rate coefficients were determined using eqn. (IX). Fig. 3 shows an example of a plot of these coefficients *vs.* C_2H_2 concentration, from which effective rate constants k^{eff} for the $OH + C_2H_2$ reaction in the presence of O_2 were

Table 3 Summary of results: HO_2-loss rate coefficients, effective rate constants of the $OH + C_2H_2$ reaction, slope (m) and intercept (b) of a correlation of effective OH loss and HO_2 formation rate coefficients, difference (d) of fitted HO_2 formation rate coefficient intercepts ($[C_2H_2] = 0$) and τ_0^{-1}, and rate constant (k_6) of the $OH + NO$ reaction

	${}^1k_{1,\text{HO}_2}$ [a]/10^3 s^{-1}	$k^{\text{eff}}/10^{-13}$ cm^3 s^{-1}	m	$-b/10^2$ s^{-1}	d [b]/s^{-1}	$k_6/10^{-12}$ cm^3 s^{-1}
			matrix gas: 5% O_2 in N_2 [c]			
1	0.70 ± 0.03	1.44 ± 0.13	1.131 ± 0.046	2.65 ± 0.40	−1 ± 52	
2	0.71 ± 0.02	1.60 ± 0.16	1.112 ± 0.023	2.85 ± 0.27	−11 ± 38	2.39 ± 0.22
3	1.13 ± 0.03	1.54 ± 0.07	1.153 ± 0.020	4.16 ± 0.23	−20 ± 23	
4	1.17 ± 0.04	1.55 ± 0.18	1.113 ± 0.041	4.20 ± 0.52	−8 ± 37	
5	0.72 ± 0.02	1.79 ± 0.13	1.022 ± 0.048	3.76 ± 0.65	6 ± 19	4.62 ± 0.32[d]
6	1.27 ± 0.02	1.83 ± 0.20	1.041 ± 0.017	6.86 ± 0.35	−9 ± 83	
7	0.97 ± 0.02	2.11 ± 0.14	1.008 ± 0.033	7.59 ± 0.81	7 ± 55	7.42 ± 0.29[d]
8	1.43 ± 0.05	2.13 ± 0.20	1.004 ± 0.045	11.45 ± 1.43	54 ± 108	
			matrix gas: O_2 [c]			
9	1.04 ± 0.02	2.73 ± 0.41	1.098 ± 0.029	1.81 ± 0.25	−28 ± 62	1.26 ± 0.07[d]
10	1.58 ± 0.04	2.49 ± 0.45	1.099 ± 0.035	2.73 ± 0.33	−2 ± 70	
11	0.75 ± 0.02	2.80 ± 0.12	1.084 ± 0.017	2.17 ± 0.21	19 ± 25	
12	0.72 ± 0.02	3.00 ± 0.19	1.061 ± 0.011	2.12 ± 0.15	−10 ± 43	2.06 ± 0.18
13	1.26 ± 0.03	2.90 ± 0.19	1.080 ± 0.010	3.27 ± 0.15	−23 ± 49	
14	1.23 ± 0.02	2.74 ± 0.11	1.079 ± 0.016	3.51 ± 0.25	13 ± 22	
15	0.76 ± 0.02	3.53 ± 0.09	1.048 ± 0.004	3.88 ± 0.09	−7 ± 45	4.14 ± 0.48[d]
16	1.45 ± 0.02	3.47 ± 0.25	1.062 ± 0.013	7.33 ± 0.36	75 ± 101	
			matrix gas: O_2 [c], CO instead of C_2H_2, k_7 instead of k^{eff}			
17	1.06 ± 0.05	1.66 ± 0.06	0.992 ± 0.007	2.46 ± 0.10	33 ± 75	2.09 ± 0.31[d]
18	1.69 ± 0.01	1.67 ± 0.11	0.983 ± 0.009	3.50 ± 0.10	4 ± 122	

Error limits are 2σ (statistical) if not stated otherwise. [a] Averaged value over N (Table 1) values, error limits reflect the largest deviation within the sets. [b] Error limits of fitted HO_2-formation rate coefficient intercepts ($[C_2H_2] = 0$). [c] 1–3% He or Ar are always present owing to the use of diluted NO. [d] Only two data points available, linear regression was forced through the origin.

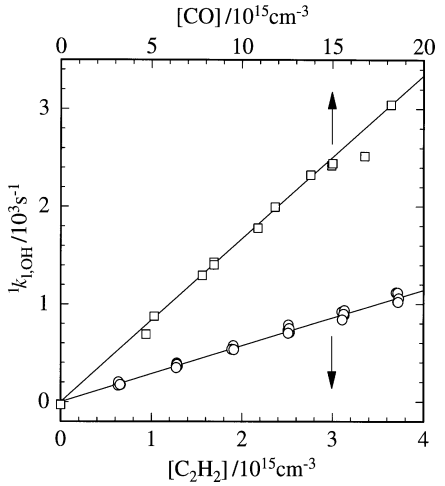

Fig. 3 OH-loss rate coefficients (effective in case of C_2H_2) as a function of C_2H_2 (○) and CO (□) concentrations at a total pressure of 20 kPa of O_2. The results of four sets with C_2H_2 (# 11–14) and all data obtained with CO are shown. Fitted intercepts, resulting from different NO and H_2O_2 concentrations, were subtracted to allow a comparison of data from different sets.

derived [eqn. (IV)]. The results are listed in Table 3. The intercepts, $c_{1,\mathrm{OH}}$, dependent on NO and H_2O_2 concentrations, as well as on total pressure, will be examined below. They were subtracted in Fig. 3 to allow a comparison of data from different sets. No effect of NO and H_2O_2 concentrations on the rate constants is noticeable. In Fig. 4 k^{eff} is plotted *vs.* total pressure. A slight pressure dependence is noticeable, while the effect of the O_2 mixing ratio on the rate constant is much more pronounced. This result is consistent with recent work on the C_2H_2 + OH reaction in the presence of O_2.[13]

By using CO instead of C_2H_2, rate constants k_7 for the reaction OH + CO were derived. Fig. 3 shows the corresponding plots in comparison with the data obtained for C_2H_2. The results are in good agreement with recent recommendations[19,21] and given in Table 3. An additional relative error of 10% on account of possible systematic errors is estimated for both k^{eff} and k_7.

HO_2 yields

The independence of HO_2-loss rate coefficients on C_2H_2 concentrations justifies the use of eqn. (XI) to obtain effective HO_2-formation rate coefficients. Plots *vs.* C_2H_2 concentrations also show linear dependences, as expected from eqn. (VI), with intercepts depending on H_2O_2 concentrations. The results of the corresponding linear regressions, *i.e.* effective rate constants of HO_2 formation, are not given separately. Instead, slopes (m) and intercepts (b) from a direct correlation of effective HO_2-formation and OH-loss rate coefficients are given,

$$^1k^{\mathrm{eff}}_{\mathrm{f,HO_2}} = m\,{}^1k^{\mathrm{eff}}_{\mathrm{l,OH}} + b \qquad \text{(XV)}$$

with the intercepts b related to the rate coefficients in the absence of C_2H_2 (CO):

$$b = c_{\mathrm{f,HO_2}} - mc_{\mathrm{l,OH}} \qquad \text{(XVI)}$$

m corresponds to the ratio of effective rate constants for HO_2 formation and OH loss *i.e.* the yield of HO_2 formed for each OH effectively consumed in reactions (1) and (2). In all cases, m is close to unity which, at a first glance, is in agreement with the proposed model [Fig. 2 and eqn. (VI)]. On the other hand, considering the small statistical error limits, most of the values obtained with C_2H_2 are significantly higher than one, while measurements with CO gave m-values very close to unity, in agreement with expectations. Fig. 5 shows examples of correlation plots, demonstrating the low scatter of the data and the significance of the differences between C_2H_2 and CO.

In Fig. 6, the HO_2 yield is plotted as a function of total pressure. There appears to be a slight pressure dependence, which is more pronounced at the lower O_2 concentration. At 100 kPa, m approaches the expected value of one. Hence, deviations from the proposed reaction model are significant only at low pressures. A possible explanation for this behaviour will be given below.

HO_2 formation in the absence of C_2H_2 (CO), and OH loss in the absence of C_2H_2 (CO) and NO are expected to be due to the OH + H_2O_2 reaction. Hence, the fitted intercepts $c_{\mathrm{f,HO_2}}$ and the directly measured values of τ_0^{-1} should be similar.

$$c_{\mathrm{f,HO_2}} = k_5[\mathrm{H_2O_2}] = \tau_0^{-1} \qquad \text{(XVII)}$$

The differences,

$$d = c_{\mathrm{f,HO_2}} - \tau_0^{-1} \qquad \text{(XVIII)}$$

are given in Table 3 with the 2σ error limits of the intercepts. In all cases, d is zero within these error limits, which again is in accordance with expectations. Measurements without C_2H_2 were made in roughly half the series. In all cases these measured values of the HO_2 formation rate coefficients at

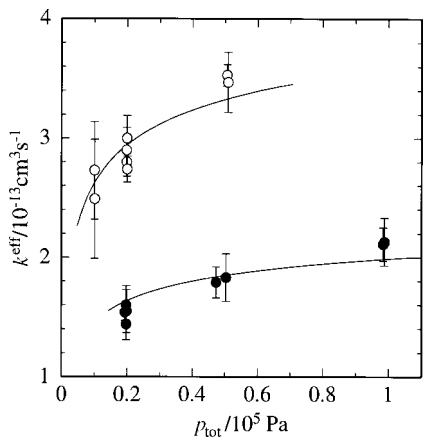

Fig. 4 Effective rate constants of the OH + C_2H_2 reaction as a function of total pressure and O_2 concentration: (●) 5% of O_2 in N_2, (○) O_2. Error bars indicate error limits from Table 3. The full lines show the pressure dependence of the rate constant of the OH + C_2H_2 reaction in N_2[13] scaled by factors of 0.25 (5% of O_2) and 0.45 (O_2).

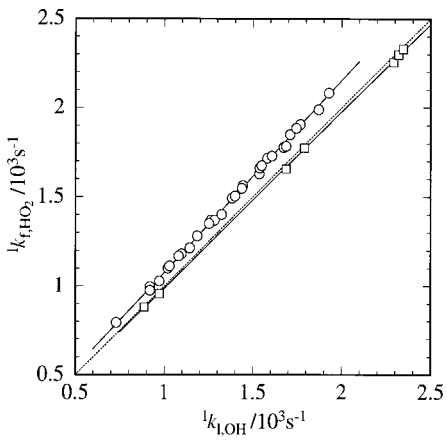

Fig. 5 Correlation of HO_2-formation and OH-loss rate coefficients (both effective in case of C_2H_2) at a total pressure of 20 kPa of O_2: C_2H_2 (# 11–14) (○), part of the CO data (□). Intercepts b from Table 3 were subtracted to allow a comparison of data from different sets. Straight lines show averages of m from Table 3 and the dashed line indicates the expected correlation (m = 1).

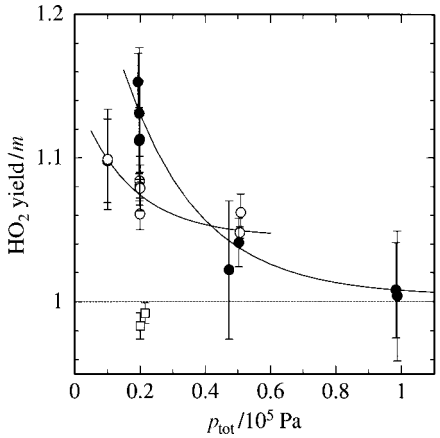

Fig. 6 Pressure dependence of the HO_2 yield for each OH effectively consumed in the OH + C_2H_2 and following O_2 reactions: 5% of O_2 in N_2 (●), O_2 (○), and results for CO, obtained in O_2 (□). The dashed line corresponds to the expected value of one, while the full lines indicate the different trends observed at different O_2 concentrations.

$[C_2H_2] = 0$ and the fitted intercepts are similar within their error limits.

Rate constants of OH + NO

Finally, the data allow rate coefficients for the terminating reaction OH + NO to be calculated from the differences of OH-loss and HO_2-formation rate coefficients in the absence of C_2H_2 (CO),

$$c_{l,\,OH} - c_{f,\,HO_2} = k_6[NO] \qquad \text{(IXX)}$$

The series performed at 20 kPa each gave four data points, allowing a linear regression to obtain k_6. The corresponding values are given in Table 3. The intercepts ([NO], $[H_2O_2] = 0$) are very close to zero, $(6 \pm 23)\ s^{-1}$ (#1–4) and $(6 \pm 20)\ s^{-1}$ (#10–13) in accordance with the estimate given in the Experimental section ($\leqslant 10\ s^{-1}$). For the series at other total pressures, where only two data points were available, fits were, therefore, forced through the origin in order to estimate the rate constants listed in Table 3. The results are in good agreement with those derived in our recent study on the HO_2 + NO reaction[18] and with current recommendations,[19,21] and will not be discussed further.

Discussion

Effective rate constants of the OH + C_2H_2 reaction

In previous work,[13] monoexponential OH-decay curves were observed in the presence of C_2H_2 and a large excess of O_2. This time-behaviour is expected when steady-state conditions are assumed for the adduct, C_2H_2OH. The corresponding effective rate constants for the OH + C_2H_2 reaction, equally defined as in this work, were found to depend on total pressure and O_2 mixing ratio. For fixed O_2 mixing ratios, almost the same fall-off behaviour was observed as in the absence of O_2. This led to the conclusion that the effective rate constants can be described by a product of a pressure-dependent addition rate constant k_{1a} (*ca.* k_1 at higher pressures), independent of O_2, and an O_2 mixing ratio dependent factor $(1 - \phi^{OH})$, independent of pressure, with ϕ^{OH} being the OH yield of the adduct + O_2 reaction (2). The observed non-linear dependence of the factor $(1 - \phi^{OH})$ on the O_2 mixing ratio was explained by different reactive properties of vibrationally excited adducts with respect to O_2.[13]

The effective rate constants derived in the present work agree with this picture. The full lines in Fig. 4 show the pressure dependence of the OH + C_2H_2 reaction in N_2,[13] scaled by factors of 0.45 (O_2) and 0.25 (5% of O_2) to fit the data. From our previous work,[13] factors of 0.43 ± 0.04 and *ca.* 0.22 are expected, respectively. Thus, the effective rate constants obtained here, in the presence of NO and derived from an analysis of a different OH time-behaviour, are similar.

HO_2 yield

Considering the proposed reaction model, the overall HO_2 yield m is given by the following expression:

$$m = \frac{\phi_1^{H}\phi_8^{HO_2} + \phi_1^{C_2H_2OH}\phi_2^{HCO}\phi_3^{HO_2}}{\phi_1^{H+CH_2CO} + \phi_1^{C_2H_2OH}(1 - \phi_2^{OH})} \qquad \text{(XX)}$$

Here, the different ϕ values denote the yields of the products (upper index) of the different reactions (lower index). The HO_2 yields of reactions (3) and (8) can be assumed to be one, because of the high O_2 concentrations employed. Moreover, at higher pressures, the yield of H-atoms (and ketene) of reaction (1), is negligible,[17] which leads to:

$$m \approx \frac{\phi_2^{HCO}}{1 - \phi_2^{OH}} \qquad \text{(XXI)}$$

Thus, in the case where there are only two reaction channels for the adduct + O_2 reaction, one regenerating OH, the other forming HO_2 *via* HCO, an m-value of one should be obtained. This is in fact observed at 100 kPa and in good approximation also for the lower total pressures.

However, deviations from this ideal value cannot be explained within the proposed model. Even if reaction (1b) is considered, m should remain one. Although m only increases slightly towards lower pressures, this increase is significant, which is reflected in the small statistical error limits given in Table 3. An error analysis considering eqn. (VIII) and (XI) reveals that fluctuations in the ratio c_1/c_2 and in τ_1 produce the largest shifts in OH-loss and HO_2-formation rate coefficients. Fortunately, these shifts go in the same directions and have almost the same magnitudes, *i.e.* they hardly influence the correlations [eqn. (XV)]. In accordance with this, it was found that the absolute statistical errors of the results of linear regressions to obtain effective rate constants for OH loss and HO_2 formation are similar (within 20%) for both slopes and intercepts. They are, therefore, not completely listed in Table 3. Moreover, while, for the rate constants, the precision of C_2H_2 (CO) concentrations is important and has been considered in the additional 10% estimate of the errors, this is not the case for m. Hence, the precision of the given values and their increase towards lower pressures is real, as long as the OH time-behaviour is really biexponential. There are indications that this is the case, especially the consistency of the data obtained with and without C_2H_2 and the constancy of the derived HO_2 loss rate coefficients (due to HO_2 + NO).

Nevertheless, as mentioned above, the measurements made with 5% O_2 at 10 kPa are inconsistent with all other sets. Under these conditions, k^{eff} is relatively small and reaction (1b) may account for *ca.* 10%.[13] At the same time, the lifetime of H atoms, produced in reaction (1b), is increased to *ca.* 60 μs,[19] probably too long for the assumption of steady-state conditions, essential for pure biexponential time-behaviour. A delayed formation of HO_2 *via* H + O_2 may appear to give a lower HO_2 loss rate coefficient, as has been observed qualitatively. This possible perturbation may already be negligible at 20 kPa and the same O_2 mixing ratio, since the lifetime of H-atoms drops to *ca.* 15 μs[19] and the contribution of reaction (1b) is expected to be lower. However, the increase in m towards lower pressures indicates that additional reactions become important which, from a certain point, may destroy the simple kinetics.

A small additional HO_2 source may be related to the OH regenerating reaction (2a). Zhang and Peeters[14] supposed that excited glyoxal may dissociate into HCO radicals:

$$C_2H_2OH + O_2 \rightarrow (CHO)_2^{\#} + OH \qquad (2a)$$

$$(CHO)_2^{\#} \xrightarrow{M} (CHO)_2 \qquad (9a)$$

$$\longrightarrow 2\ HCO \qquad (9b)$$

In the present system this would, indeed, lead to additional HO_2 formation, not related to an effective loss of OH. The corresponding expression for m now allows values higher than one:

$$m = \frac{\phi_1^{H} + \phi_1^{C_2H_2OH}(\phi_2^{HCO} + \phi_2^{OH}\phi_9^{HCO})}{\phi_1^{H+CH_2CO} + \phi_1^{C_2H_2OH}(1 - \phi_2^{OH})} \approx \frac{\phi_2^{HCO} + \phi_2^{OH}\phi_9^{HCO}}{1 - \phi_2^{OH}} \qquad (XXII)$$

In the right-hand side of this equation reaction (1b) has been omitted as in eqn. (XXI). The highest value of m observed, *ca.* 1.13 at 20 kPa and 5% O_2, corresponds to an HCO yield of reaction (9) of 0.043, *i.e.* only some 2% of the glyoxal formed in reaction (2a) must dissociate to produce this effect. At the same total pressure, a slightly higher HCO yield of 0.065 is calculated, from the m-value, of *ca.* 1.08 obtained in O_2.

The energy released in reaction (2a) (-299 kJ mol^{-1})[19,22] is almost the same as the dissociation energy of glyoxal (296 kJ mol^{-1}).[19,22] From this point of view, a strong pressure dependence of a possible glyoxal dissociation can be expected and may be the reason for the observed pressure dependence of the overall HO_2 yield.

In our previous work[13] we proposed that the fraction of vibrationally excited adducts, formed from OH and C_2H_2, which reacts with O_2, increases with the O_2 mixing ratio. Higher internal energy of the reacting adduct may, therefore, also explain a stronger dissociation of glyoxal at higher O_2 mixing ratios, as indicated by the higher HCO yield given above.

As described in the Results section, the amount of NO consumed in the radical chain is considerable. The amount of NO_2 formed is almost the same and can be calculated integrating the right-hand term of eqn. (XII),

$$\frac{d[NO_2]}{dt} = k_4[HO_2][NO] \qquad (XXIII)$$

which leads to:

$$\frac{\Delta[NO_2]}{[OH]_0} \approx (\tau_2 - \tau_1)\frac{c_1/c_2(\tau_1^{-1} - \tau_2^{-1})}{(1 + c_1/c_2)^2} \qquad (XXIV)$$

The approximation means that the NO concentration is assumed to be constant in the integration and that OH-formation and HO_2-loss rate coefficients are taken to be similar [eqn. (V)]. Taking the measurements of Table 2 as an example, the ratio given by eqn. (XXIV) is *ca.* 19 for the highest C_2H_2 concentration. This ratio drops to *ca.* 7 in the case of CO or H_2O_2 under the same conditions and similar OH-loss rate coefficients. Thus, formation of NO_2 is a very sensitive measure of any additional source of radicals, since this source is amplified by the radical chain. Note, that absolute values of $[OH]_0$ are known here from the attenuation of the analysing laser beam by the pressure-broadened[23] $Q_1(2)$ line of the OH (X–A) transition at known path length.

Addition of CO and NO to a gas sample, and detection of the NO_2 formed in the resulting reaction chain, is a means of monitoring RO_x radicals. Recently, measurements have been made where CO and acetylene were compared in such a set-up, while maintaining a constant concentration of HO_2 radicals in the probed gas stream.[24] At a total pressure of 1 bar of synthetic air, the amount of NO_2 formed using acetylene was increased by *ca.* 20% compared with CO. This result can be explained by no more than a 0.75% dissociation of glyoxal under these conditions,[24] which is in line with the results of this work.

Conclusion

The HO_2 yield of secondary processes following OH reaction with acetylene in the presence of O_2 has been determined as a function of total pressure and O_2 mixing ratio. The results are in good agreement with the reactive pathways proposed by Hatakeyama *et al.*[17] for the reaction of acetylene–OH adducts with O_2, namely glyoxal + OH and formic acid + HCO, and with earlier results on the O_2 mixing ratio dependence of the OH yield of this reaction.[13] The observed decrease in the OH-forming channel with O_2 mixing ratio is found to be balanced by an increase of the HCO-forming channel. Deviations from this simple scheme have been observed at lower total pressures. While these are not thought to have implications for the atmospheric degradation of acetylene, they appear to be increasingly important at low pressures and hint at an interesting net production of radicals under low-pressure conditions. A pressure- and O_2 mixing ratio-dependent dissociation of a small fraction of vibrationally excited glyoxal from the acetylene–OH adduct + O_2 reaction is proposed to account for this additional radical source.

Support of this study by the Bundesminister für Wissenschaft, Bildung, Forschung und Technologie (BMBF), grant 07TFS30/D3, is gratefully acknowledged.

References

1 R. Atkinson, *J. Phys. Chem. Ref. Data*, Monograph 1, 1989, 121.
2 R. A. Perry, R. Atkinson and J. N. Pitts Jr., *J. Chem. Phys.*, 1977, **67**, 5577.
3 J. V. Michael, D. F. Nava, R. P. Borkowski, W. A. Payne and L. J. Stief, *J. Chem. Phys.*, 1980, **73**, 6108.
4 R. A. Perry and D. Williamson, *Chem. Phys. Lett.*, 1982, **93**, 331.
5 G. P. Smith, P. W. Fairchild and D. R. Crosley, *J. Chem. Phys.*, 1984, **81**, 2667.
6 J. A. Miller and C. F. Melius, in *Twenty-Second Symposium (International) on Combustion*, The Combustion Institute, Pittsburgh, PA, 1988, p. 1031.
7 V. Schmidt, G-Y. Zhu, K. H. Becker and E. H. Fink, in *Physico-Chemical Behaviour of Atmospheric Pollutants*, ed. B. Versino and G. Angeletti, Reidel, Dordrecht, 1984, p.177.
8 A. Wahner, Dissertation, Universität Bochum, 1984.
9 A. Wahner and C. Zetzsch, *Ber. Bunsen-Ges. Phys. Chem.*, 1985, **89**, 323.
10 V. Schmidt, G. Y. Zhu, K. H. Becker and E. H. Fink, *Ber. Bunsen-Ges. Phys. Chem.*, 1985, **89**, 321.
11 E. H. Fink and V. Schmidt, Bericht Nr. 8, Fachbereich 9, Universität Wuppertal, 1985.
12 M. Siese and C. Zetzsch, *Z. Phys. Chem.*, 1995, **188**, 75.
13 B. Bohn, M. Siese and C. Zetzsch, *J. Chem. Soc., Faraday Trans.*, 1996, **92**, 1459.
14 Z. Y. Zhang and J. Peeters, in *Physico-Chemical Behaviour of Atmospheric Pollutants*, ed. Restelli and G. Angeletti, Kluwer Academic Publishers, Dordrecht, 1990, p. 377.
15 J. R. Kanofsky, D. Lucas, F. Pruss and D. Gutman, *J. Phys. Chem.*, 1974, **78**, 311.
16 W. Hack, K. Hoyermann, R. Sievert and H. Gg. Wagner, *Oxid. Commun.*, 1983, **5**, 101.
17 S. Hatakeyama, N. Washida and H. Akimoto, *J. Phys. Chem.*, 1986, **90**, 173.
18 B. Bohn and C. Zetzsch, *J. Phys. Chem.*, 1997, **101**, 1488.
19 W. B. DeMore, S. P. Sander, D. M. Golden, R. F. Hampson, M. J. Kurylo, C. J. Howard, A. R. Ravishankara, C. E. Kolb and M. J. Molina, in *Chemical Kinetics and Photochemical Data for Use in Stratospheric Modeling*, Evaluation Number 12; JPL Publication 97-4, Jet Propulsion Laboratory, Pasadena 1997, and references therein.
20 A. Wahner and C. Zetzsch, *J. Phys. Chem.*, 1983, **87**, 4945.

21 R. Atkinson, D. L. Baulch, R. A. Cox, R. F. Hampson Jr., J. A. Kerr, M. J. Rossi and J. Troe, *J. Phys. Chem. Ref. Data*, 1997, **26**, 577; 580; 617.
22 J. D. Cox and G. Pilcher, in *Thermochemistry of Organic and Organometallic Compounds*, Academic Press, London, 1970.
23 C. Zetzsch and C. Leonard, in *Proc. EUROTRAC Symposium '90*, ed. P. Borrell, P. M. Borrell and W. Seiler, SPB Academic, The Hague, 1991, p. 483.
24 M. Elend and C. Zetzsch, in *Proc. 1st Workshop of the EUROTRAC-2 Subproject Chemical Mechanism Development (CMD)*, ed. M. Ammann and R. Lorenzen, ETH-Zürich/Paul Scherrer Institute, Villigen, 1997, p. 135.

Paper 7/08536B; *Received* 26*th November*, 1997